Impact of Fuel and Injection System on Particle Emissions from a GDI Engine

Wang, Chongming; Xu, Hongming; Herreros, Jose; Wang, Jianxin; Cracknell, Roger

DOI:
10.1016/j.apenergy.2014.06.012

Document Version
Peer reviewed version

Citation for published version (Harvard):
Wang, C, Xu, H, Herreros, J, Wang, J & Cracknell, R 2014, 'Impact of Fuel and Injection System on Particle Emissions from a GDI Engine', *Applied Energy*, vol. 132, pp. 178-191.
https://doi.org/10.1016/j.apenergy.2014.06.012

Impact of Fuel and Injection System on Particle Emissions from a GDI Engine

Chongming Wang[1], Hongming Xu[1,2], Jose Martin Herreros[1], Jianxin Wang[2], Roger Cracknell[3]*

1. University of Birmingham, Birmingham, UK

2. State Key Laboratory of Automotive Safety and Energy, Tsinghua University, Beijing

3. Shell Global Solutions, UK

Abstract

In recent years, particulate emissions from the gasoline direct injection (GDI) engine, especially the ultrafine particulates, have become a subject of concern. In this study, the impact of fuel (gasoline versus ethanol) and injection system (injection pressure and injector condition) on particle emissions was investigated in a single cylinder spray-guided GDI research engine, under the operating conditions of stoichiometric air/fuel ratio, 1500 rpm engine speed and 3.5-8.5 bar IMEP. The results show that, in a spray guided GDI engine, ethanol combustion yields much lower particle mass (PM) but higher particle number (PN) emissions, compared to gasoline. Depending on the fuel used, the PM and PN emissions respond differently to injection pressure and injector condition. For gasoline, the injection system has a significant impact on the PM and PN emissions. High injection pressure and clean injector condition are both essential for low particle emissions. Compared to gasoline, the particle emissions from ethanol combustion is less sensitive to the injection system, due to its higher volatility and diffusive combustion which produces less soot. Furthermore, a PM and PN trade-off was observed when using gasoline and ethanol, and when using high injection pressures.

Keywords: Particulate matter; Injector fouling; Injection pressure; GDI

* To whom correspondence should be addressed. Email: h.m.xu@bham.ac.uk

1. INTRODUCTION

Vehicles powered by gasoline direct injection (GDI) engines aiming to improve engine efficiency and reduce fuel consumption have entered the car market since the late 1990s [1-6] and the global volume of GDI engines is expected to overtake that of port fuel injection (PFI) engines by 2020 [7]. Significant reduction of pollutant emissions in SI engines has been achieved in the past decade by using various advanced technologies like direct injection (DI), exhaust gas recirculation (EGR), variable valve timing, stratified-charge combustion, clean fuels such as bio-ethanol and high efficient three-way catalysts (TWCs) [8-11]. Some other technologies such as turbochargers which are usually used in diesel engines are also potentially used to increase engine efficiency and therefore reduce emissions [12, 13].

Historically, particulate emissions have been related to diesel engines [14-16]. However in recent years, particulate emissions from the gasoline direct injection (GDI) engines, especially the ultrafine particulates, have become a subject of concern. Research evidence shows that the particle mass (PM) and particle number (PN) emissions from GDI engines are similar in level or even higher than those of the diesel engines equipped with diesel particulate filters (DPFs) [17-21]. As a result of environmental and health concerns [22], the Euro 5b regulations, limit the PM emissions from vehicles equipped with GDI engines. The coming new emission legislations will, for the first time, set limits not only on mass, also on number of particulates.

The particulate emissions from GDI engines should be addressed through either the combustion process or after-treatment systems. Therefore, it is of vital importance to understand the characteristics of particulates (i.e. nature, size, morphology, structure, etc.) as well as the influence of different factors on their formation/oxidation mechanisms, which includes the engine type, fuel properties, and injection system.

Engine type shows a direct link to the particle emissions. Research evidence shows that particles from the wall-guided and spray-guided GDI engines demonstrate significantly different characteristics. Andersson et al. studied PM emissions from wall-guided GDI engines and found that elemental soot was the most abundant component (72%) in its composition, which is similar to that of diesel engines [23]. Price et al. [24]

investigated PM emissions from a spray-guided GDI engine, and concluded that the particle composition was dominated by volatile organic materials whilst the elemental carbon/soot fraction accounted for at most 2%-29% of its composition, depending on the injection pressure, air/fuel ratio and start of injection. The difference mentioned above is because of the differences in the air-fuel mixture preparation for wall-guided and spray-guided engines. Unlike wall-guided GDI engines, spray-guided GDI engines have less fuel impingement on the piston crown; therefore the combustion is less diffusive.

The particle emissions vary widely, depending on fuel properties such as aromatic content, volatility and oxygen content [25-31]. The fuel volatility is directly linked to air/fuel mixture preparation and thus particle emissions [32]. Liquid fuels like iso-octane produce more PM emissions than gaseous fuels such as propane [33]. Aikawa et al. [25]suggested that fuel vapour pressure and fuel structure (double bond and aromatic ring) play important roles in the PM formation. A 'PM Index' for predicting PM emissions in gasoline vehicles was proposed. They calculated the PM Index distribution of 1445 commercially available gasoline fuels from around the world and found that the PM Indices of gasoline fuels sold globally fall in a very wide band. Leach et al. [34] studied the influence of fuel properties on PN emissions from a GDI engine, by designing fuels with differing volatility and aromatic content, and validated a 'PN index' for evaluating the PM emissions from commercial gasoline fuels. It is well reported that compared to gasoline, pure ethanol produces much less PM emissions in GDI engines [27, 35, 36]. The effect of ethanol blending levels in gasoline on PM emissions in the GDI engine is not well understood. Mohammad et al. reported a significant reduction of soot formation by using alcohol blends [37], which is supported by other publications [38-41]. However Chen et al.'s data show that increases in both PM and PN emissions were observed with ethanol addition, particularly in a cold engine [26]. Other publications also concluded that a low ethanol-gasoline blend had higher or similar PM emissions compared with pure gasoline [27, 32, 36, 42].

Injection system parameters, such as the injection pressure and injector condition, are important in determining the engine-out PM characteristics. Higher DI injection pressure leads to higher spray velocity,

shorter injection pulse and smaller droplets which are more widely distributed [43]. He et al. studied various injection pressures (33-68 bar) in a wall-guided GDI engine and found that a high injection pressure reduced PN emissions [44]. Matousek et al. [45] investigated DI injection pressure in a single-cylinder GDI engine and found that the PN emission was reduced by 70% using 200 bar instead of 100 bar injection pressure, and was reduced by another 50% by using 300 bar injection pressure.

Injector conditions affect the quality of spray and atomisation directly [1, 46], and thus they subsequently affect the engine-out emissions [46-49]. Injector fouling in GDI engines is a far greater concern than in PFI engines due to the injectors' harsher thermal conditions and its direct impact on the fuel and air mixture process, and combustion [1, 47, 50, 51]. A fouled injector is expected to cause issues. For example spray quality will be reduced leading to poor local mixing, the injector nozzles can be blocked reducing flow which could lead to Engine Management System (EMS) trim and set-point changes, and uneven flow between holes can occur leading to misdistribution in the cylinder (lean / rich regions). It is reported that a fouled injector with a 22% fuel flow rate lose led to 30% and 190% more HC and CO emissions respectively compared to a clean injector [52]. Similar results were also observed in [53]. There are limited publications concerning the impact of injector condition on particle emissions in GDI engines. Berndorfer et al. [54] studied a fouled injector and observed diffusion combustion phenomenon near the injector tip, after the main combustion in a GDI optical engine, leading to high soot and high HC emissions.

Injector deposit formation is found to be closely related to the injector tip temperature [46, 48, 53, 55, 56]. By carefully designing the combustion system, the tendency of injector deposit formation can be reduced. For example, the injector tip temperature is affected by 1) protrusion of its tip into the cylinder, 2) conductive path from the injector mounting socket to the coolant passage, and 3) in-cylinder charge velocity near the tip location. The position of the injector relative to the spark plug is another critical feature; the longer the distance, the lower the injector nozzle temperature tends to be [46, 55, 57]. Increasing fuel injection pressure is also an effective way of controlling GDI injector deposit formation [48, 55].

Based on the literature study, it can be concluded that there is an increasing interest in understanding the PM characteristics of GDI engines, but detailed investigations of the effect of fuel and injection system are limited, especially concerning spray-guided GDI engines. Even through it is clear that gasoline fuel and injection pressure both have significant impact on the particulate emissions in GDI engines, it is not clear which of those two factors is more prominent. Therefore, this paper examines the impact of fuel and injection system on PM emissions in a spray-guided GDI engine. Two fuels (gasoline and ethanol), four injection pressures (50, 100, 150 172 bar) and three injectors (one clean injector and two fouled injectors) were tested. The test conditions were stoichiometric air-fuel ratio, 1500 rpm engine speed and 3.5-8.5 bar IMEP engine load.

2. EXPERIMENTAL SYSTEMS AND METHODS

2.1. ENGINE AND INSTRUMENTATION

The specifications of the single cylinder GDI research engine used in this study are listed in Table 1 and its experimental system is shown in Figure 1. The engine was coupled to a direct current (DC) dynamometer to maintain a constant speed (±1 rpm) regardless of the engine torque output. The in-cylinder pressure was measured using a Kistler 6041A water-cooled pressure transducer. All temperatures were measured with K-type thermocouples. Coolant and oil temperatures were maintained at 358 K and 368 K (±3 K) respectively, using a Proportional Integral Differential (PID) controller and heat exchangers. A 100 L intake buffer tank was used to stabilize the intake air flow.

The engine was controlled using an in-house control software written in LabView. The HC emissions were measured using a Horiba MEXA-7100DEGR gas Analyser with a resolution of 1 ppm. Exhaust samples were taken 0.3 m downstream of the exhaust valve and pumped via a heated line (maintained at 464 K) leading to the gas Analyser. The PM emission was measured using a Scanning Mobility Particle Sizer Spectrometer (SMPS3936) supplied by TSI. PM samples were taken 0.33 m downstream of the exhaust valve

via a rotational disk dilution system supplied by TSI. The sampling head was maintained at 425 K, the highest setting available for the rotational disk dilution system. A dilution ratio of 50 was set in this study.

2.2. INJECTOR AND FLOW RATE TEST

The injectors used in this experimental study include two GDI injectors which were used in previous engine experiments in the Future Engines and Fuels Lab at Birmingham, using various fuels for about 3 months under engine load conditions ranging from 3.5 to 8.5 bar IMEP. Carbon deposits were accumulated in the injector nozzle and also on the injector tip. To quantitatively characterise the status of the two injectors, their flow rates were measured on a test bench with 150 bar injection pressure using iso-octane as the test fuel. Ten injection pulse widths ranging from 0.3 to 6 ms were selected, and the fuel from 1000 injections was quantitatively measured by a balance with a resolution of 0.1 g. All the measurements were repeated at least three times and the averaged results were used to calculate the flow rate loss, shown in Figure 2. Injector 1 showed a flow rate loss of 8.5%, and injector 2 showed a flow rate loss of 5.3%. Injector 3 is the clean injector used as the benchmark. After the flow rate test, the injectors were used to study of the effect of injector fouling on the PM emissions.

It is important to maintain the injector condition consistently throughout the PM measurement, and thus the possibility that injector deposits are washed away or further accumulated during the present experimental investigation has been considered. The variation in injection pulse width for a certain injection quantity was used as a simple indicator of the variation of injector condition. The engine test designed for the study of the effect of a fouled injector on PM emissions lasted 3 hours for each injector. Each engine operating point (3.5-8.5 bar IMEP) was repeated at least three times and the injection pulse width was recorded. There was no evidence that injector 1 and 2 experienced any noticeable change during the PM measurement in this study. Figure 3 shows the injection pulse width of injector 1 throughout the PM measurement. It is clear that the

injection pulse width in the 3 tests had very good repeatability and therefore, it is believed that the injector conditions throughout the experimental study were consistent.

In summary, although the injectors were not fouled using a bespoke technique, the level of flow loss in each injector has been accurately characterised, and it has been shown that the level of flow loss has remained consistent throughout the experimental study.

2.3. PM MASS CALCULATION

In this paper, PN was directly measured by using SMPS. PM mass was calculated from PN by using Equation (1) [58], which is developed by Cambustion Ltd., University of Oxford and University of Manchescter .

$$\mathrm{Mass_{agg}} = 1.72 * \mathrm{n_{agg}} * {\mathrm{d_p}}^{2.65} * 10^{-24} \qquad \text{Equation (1)}$$

where $\mathrm{d_p}$represents the aggregated particle diameter; $\mathrm{n_{agg}}$ represents the number of aggregate particles at the diameter of $\mathrm{d_p}$, which is the PM size distribution measured by SMPS; $\mathrm{Mass_{agg}}$ represents PM mass of aggregated particles at the diameter of $\mathrm{d_p}$.

2.4. EXPERIMENTAL PROCEDURE

The gasoline and ethanol used in this study have the properties listed in Table 2 and they were supplied by Shell Global Solutions (UK) without any performance additives. The test matrix is listed in Table 3. The engine was firstly warmed up with the coolant and lubricating temperatures stabilized at the selected conditions for the fixed engine speed of 1500 rpm, which was controlled by the DC dynamometer. The engine speed of 1500 rpm is the engine speed used at the Ford worldwide mapping point. All of the tests for each fuel carried out in this work were done under the fuel-specific optimum spark timings [35], known as the maximum brake torque (MBT) timings. Spark sweeps were performed for each fuel at various loads (3.5-8.5

bar IMEP at 1 bar IMEP intervals). On the boundary of knocking or combustion instability (COV of IMEP > 5%), the MBT timing was retarded by 2 CAD. In such cases, the optimum ignition timing is referred to as the knock-limited spark advance (KLSA) [35]. The engine load ranging from 3.5 to 8.5 bar IMEP was controlled by adjusting both the injection pulse width and throttle position while keeping the air/fuel ratio at stoichiometric condition. After the specific engine load was stabilized, the PM size distribution and HC emissions were measured by the SMPS and Horiba MEXA-7100DEGER respectively. In-cylinder pressure and exhaust temperature were monitored as indicators of engine stability. For each operating point, three to five measurements were made and the averaged data was presented.

3. RESULTS AND DISCUSSION

The results and discussion are divided into two sections, injection pressure and injector condition (fouled/clean). In each section, the results for both gasoline and ethanol are presented. For all the particulate size distributions, ordinates of the graphics were normalized by the differential logarithm interval of the particulate size. The data have been corrected by the dilution ratio factor set in the sampling and dilution system.

3.1. IMPACT OF INJECTION PRESSURE

3.1.1. GASOLINE

Figure 4 presents the effect of injection pressure on the HC emissions for gasoline at 3.5-8.5 bar IMEP. Higher injection pressure consistently led to decreased HC emissions within the entire tested load range, resulting from improved spray quality atomization [44, 45]. Figure 5 shows the effect of injection pressure on particle size distributions in number (a, b and c) and mass (d, e and f) for gasoline at 4.5, 6.5 and 8.5 bar IMEP. At 4.5 bar IMEP, the particulate size distributions in number (Figure 5 (a)) and mass (Figure 5 (d)) had mono-peak shapes under 100-172 bar injection pressure, indicating that most of the particles were nuclei HCs and there were limited soot emissions. At 6.5 bar IMEP, the differences in particulate size distributions in

number (Figure 5 (b)) were limited, however there were obvious differences in particulate size distributions in mass (Figure 5 (e)). At 8.5 bar IMEP, both the particulate size distributions in number (Figure 5 (c)) and mass (Figure 5 (f)) demonstrated dual-modal shapes and had completely different characteristics under various injection pressures.

Particle size distributions are composed of particles with different nature: (a) nuclei HCs which mainly compose the nucleation mode, and (b) soot agglomerates with HCs condensed or adsorbed on their surface, which compose the accumulation mode [59]. Injection pressure affects particle size distributions through its impacts on both HCs and soot formation and the interactions between them. The interactions could be clearly observed in the particle size distributions in number at 8.5 bar IMEP (Figure 5 (c)). An increased injection pressure resulted in increased PN in the nucleation mode. However, at 8.5 bar IMEP, higher injection pressure contributed to lower HC emissions (Figure 4), and lower soot emissions as indicated by the lower PN at the accumulation mode. The opposite trend is because soot not only directly determines the accumulation mode, but also has an indirect impact on the nucleation mode [59]. High injection pressure reduced the soot formation and thus the available soot surface area for the HC adsorption or condensation, favouring hydrocarbon nucleation [59]. Since the nucleation mode is the main contributor of PN emissions and the accumulation mode is the main contributor of PM emissions, it can be seen that there is an apparent trade-off in the PM and PN emission in the GDI engine at high injection pressures. This example reflects the complexity of particle emission analysis, necessitating separating/identifying of particles based on the particle nature.

The separation of particles from GDI engines into the nucleation and accumulation mode is not straightforward. Previous research shows that majority of particulates from GDI engines is composed of volatile material (unburnt HCs and lubricant) while soot only accounts for a small fraction (2%-29%), depending on the engine load, injection pressure, air/fuel ratio and start of injection [24]. There is no standard method to separate the nucleation and accumulation mode based on the particle nature, due to the complexity

of particulate formation in the combustion process and evolution in the exhaust system. In most publications, particles were not classified into different modes, and analysis was done on total particle number and mass [44, 60-63]. In some publications [35, 64, 65], particle size was used to separate PM modes, with 50-100 nm corresponding to the accumulation mode and 0-50 nm corresponding to the nucleation mode, as originally proposed by Kittelson [59]. Eastwood suggested that the nucleation mode is in the size range of less than100 nm and the accumulation mode is in the range of 100-900 nm [66]. Obviously, particle size only partially reflects the particle nature; therefore we consider more interesting try to separate particulate by nature rather than just by size.

In this study, PM modes are separated based on the inflection point of the net particle size distribution using a Matlab script developed by the University of Castilla-La Mancha, which is also used in [67]. This Matlab script has its limitation that it is only able to separate the PM modes if PM size distributions have dual-modal shapes with clear separated peaks or lightly/medium overlapped peaks. The PM size distribution is the sum of the nucleation and accumulation modes. For PM size distributions that are able to be separated by this Matlab script, an assumption is made that PM size distributions for the nucleation and accumulation mode are normal distributions. The left-side of the first peak of the PM size distribution is mostly from the nucleation mode and the right-side of the second peak is mostly from the accumulation mode. The separation point and lognormal fitted distributions are based on the criteria to minimise the difference between the distribution resulting to add the two fitted log-normal distributions (i.e. nucleation and accumulation) and the actual one.

At low engine loads, the nucleation mode in the particle size distribution overlaps largely with the accumulation mode, making the separation impossible. Only in some cases such as Figure 5 (c)), a dual-mode shape with a light overlap is observed and the separation can be easily made, which is presented in Figure 6 (a). In this operating condition, the high soot concentration increased the weight of PN in the accumulation mode and reduced that in the nucleation mode, which led to two clearly separated modes. However, when soot formation is low, separation based on the particle size distributions expressed in number becomes difficult (e.g. 50 bar injection pressure and 6.5 bar IMEP, Figure 6 (d)).

Another approach to identify PM modes is proposed here. As the accumulation mode is the primary source of PM emissions, particle size distributions in mass could help to separate the modes. At 6.5 bar IMEP and high injection pressure, the particle size distribution expressed in mass had a dual-modal shape with a slight overlap (Figure 6 (d)). In this engine condition, there was a relatively low soot formation and lower HC emissions, compared with those of the lower injection pressure.

Table 4 and Table 5 list the possibility of particle mode separation based on particle size distributions in number and mass respectively. It can be concluded that high soot formation at high engine loads was the key for separation based on the particle size distribution in number, while at medium level of soot formation (such as 6.5 bar IMEP), the separation based on the particle size distribution in mass is possible.

By combining the information from Table 4 and Table 5, it is possible to study the effect of injection pressure on different types of particle mode independently, the result of which is presented in Figure 7. Increased injection pressure led to reductions of both PM and PN emissions in the accumulation mode. However, high injection pressure seemed to have a negative effect on PN emissions in the nucleation mode. The injection pressure of 172 bar consistently led to increased PN emissions in the nucleation mode compared to other tested injection pressures. This could be related to the reason mentioned earlier: low soot formation leads to less soot surface available for HCs to be condensed or adsorbed on.

3.1.2. ETHANOL

Figure 8 shows the effect of injection pressure on HC emissions for ethanol at 3.5-8.5 bar IMEP. Unlike from gasoline combustion, HC emissions from ethanol combustion were not sensitive to injection pressure. The explanation is that ethanol has a 34.8% gravimetric oxygen content, which gives it an advantage of lower soot formation compared with gasoline, due to more complete combustion and more post-flame oxidation [26, 27]. On the other hand, even though low injection pressure led to more fuel impingement on the piston and cylinder liner, ethanol evaporated more easily due to its lower boiling point compared with gasoline. Figure 9

shows the effect of injection pressure on the particulate size distributions in number (a and b) and in mass (c and d) for ethanol at 4.5 and 8.5 bar IMEP. For all tested load and injection pressure conditions of ethanol, the particle size distributions consistently demonstrated mono-peaks, with the majority of particles in the range of 30-50 nm, suggesting that the soot formation in ethanol combustion is limited.

Figure 10 shows the comparison of PM and PN emissions from gasoline and ethanol combustion under 150 bar injection pressure. Compared with the PM emissions, the PN emissions are less sensitive to fuel. The differences between the two fuels in the PN emissions are in the range of 6-16% whilst the difference in the PM emissions is about 3% at low load (3.5 bar) and up to 900% at high load (8.5 bar). The reason why ethanol has lower PM emissions compared to gasoline is due to ethanol's oxygen content and high volatility. The higher PN emissions from ethanol compared to gasoline is because of the following two reasons. Firstly, while soot as nuclei provides the surface on which unburnt HC is adsorbed or condensed, ethanol has reduced soot particles and therefore most of the HC is formed from the particles in nucleation mode, which is the main contributor to the ethanol PN emissions. Secondly, the ethanol adsorbed on the soot has higher volatilities, compared to typical HCs in gasoline, and thus the PN emissions from ethanol combustion are higher.

The differences in PM emissions made by different fuels are closely related to the fuel spray atomization and combustion process. The previous modelling study using an in-house KIVA 3V GDI engine model shows that insufficient mixing time and significant spray-wall interaction are the main reasons for poor fuel/air mixture preparation [68], which is the cause of high PM emissions in GDI engines. Engine tailpipe PM emissions are affected by the cylinder temperature and fuel composition for PM formation and oxidation. Even through ethanol sprays have lower velocities and greater sauter mean diameters (SMD) compared to gasoline [69], the oxygen content (50% by mass) in ethanol leads to less soot formation compared to gasoline. On the other hand, the availability of oxygen in ethanol also significantly encourages soot oxidation. It has been reported that the soot produced from ethanol combustion is easier to be oxidised than soot produced by gasoline combustion [70].

3.2. IMPACT OF INJECTOR FOULING

There are limited publications investigating the effect of GDI injector fouling on PM emissions, although many evidence show that fouled injector led to deteriorated fuel/air mixture preparation in GDI engines [52, 54, 71]. Therefore, in this study, quantitative results on the effect of injector fouling on PM emissions in a GDI engine are reported. High ethanol blends in the literature had lower PM emissions and were reported as giving less GDI injector fouling [40, 72-74], and at the same time it is expected that the characteristics of ethanol spray result in a different impact on mixture preparation with fouled injectors. Therefore it is of interest to examine quantitatively how PM emissions from the ethanol fuelled GDI engine responds to injector fouling.

3.2.1. GASOLINE

Figure 11 presents the effect of a fouled injector on HC emissions for gasoline at 3.5-8.5 bar IMEP at 150 bar injection pressure. Compared with the clean injector (#3), the fouled injector (#1) yielded approximately 10% higher HC emissions at the engine load range of 5.5-8.5 bar IMEP. Similar results are also reported in other publications [52, 53]. This is possibly linked to the increased fuel impingement due to longer injector pulse width resulting from injector fouling. The fuel film continues to evaporate during the combustion stroke and therefore diffusive combustion occurs, which leads to high HC and soot formation. Another reason is possibly related to the gasoline adsorbed on carbon deposits near the injector tip. The adsorbed gasoline contributes to the diffusive combustion after the main combustion, which is reported in [54] using optical diagnostics. The distorted spray which leads to imperfect air/fuel mixture preparation is also another reason for high HC emissions [1, 47, 50, 51].

Figure 12 shows the impact of injector fouling on the particulate size distributions in number (a, b and c) and mass (d, e and f) for gasoline at 4.5, 6.5 and 8.5 bar IMEP under 150 bar injection pressure. The clean injector (#3) consistently had better particulate size distributions in number and mass. At 4.5 and 6.5 bar

IMEP, it is clear that the fouled injector (#1) produced significantly higher particulate size distributions in number. At 8.5 bar IMEP, the benefit of the clean injector (#3) regarding particulate size distributions in mass is obvious.

The particulates at 6.5-8.5 bar IMEP were separated into the nucleation and accumulation modes, using the same method described in the section 3.1.1. Figure 13 presents the impact of injector fouling on PM and PN emissions at 6.5-8.5 bar IMEP at 150 bar injection pressure. At all tested engine loads, the clean injector 3 (#3) consistently led to the lowest PM and PN emissions. The high PM and PN in the accumulation mode for the fouled injector is the direct indicator of high soot formation, which is a result of diffusive combustion. Increased fuel impingement, gasoline adsorption on the deposit on the injector tip, and distorted spray all contribute to the diffusive combustion. The maximum difference was observed at the highest engine load 8.5 bar IMEP, in which the PN emissions of the clean injector (#3) were nearly 53% and 58% of those of the fouled injectors (#1) and (#2) respectively.

Figure 14 shows combustion parameters such as peak in-cylinder pressure, combustion initiation duration (CID), and combustion duration for injector (#1) and (#3) at 3.5-8.5 bar IMEP and 150 bar injection pressure. The CID is defined as the crank angle interval between the start of spark discharge and 5% mass fraction burned (MFB). The combustion duration is defined as the crank angle interval between 10% and 90% of MFB. The definition of MFB is the accumulated released heat in successive crank angle ranging from the start to the end of combustion divided by the total released heat in the whole combustion process [23]. The heat release rate is calculated using the following equation [75].

$$dQ/d\theta = \gamma/(\gamma - 1) * P * dV/d\theta + 1/(\gamma - 1) * V * dP/d\theta \qquad \text{Equation (2)}$$

where heat capacity ratio (γ) is the ratio of specific heats (C_p/C_v); θ is the crank angle; Q is the released heat; P and V are the pressure and cylinder volume.

Unlike PM emissions, those combustion parameters are not significantly sensitive to the fouled injectors, therefore, only results from injectors (#1) and (#3) are presented. It is clear that for the fouled injector (#1) the peak pressure is slightly increased by up to 0.7 bar for the engine load range of 3.5-8.5 bar IMEP, resulting from its slightly longer combustion duration (by up to 0.5 CAD). However, there is almost no difference in CID between injectors (#1) and (#3).

Figure 15 shows the comparison of PM and PN emissions for injectors (#1) and (#3) under 150 and 50 bar injection pressure at 6.5-8.5 bar IMEP. Compared with the fouled injector (#1) at 50 bar injection pressure (the worst injection system), the clean injector (#3) at 150 bar injection pressure (the best injection system) led to a reduction of the PM emission by 80.3-88.2%. This demonstrates how much difference the condition of the injection system can make to the particle emissions from the gasoline engine.

It is known that variations of fuel specifications on the market lead to variations of PM emissions from gasoline fuelled vehicle engines [25, 29, 32]. Aikawa et al. [25] proposed a 'PM index' for predicting the PM emissions for gasoline vehicles (Equation 3).

$$\text{PM Index:} \qquad I\,(VP, DBE) = \sum_{i=1}^{n}(DBE_i + 1)/(VP\_443\ K)_i)] \times W_{ti} \qquad \text{Equation (3)}$$

Here, *VP_443 K* means vapour pressure of a single component *i* at the temperature of 443 K. W_{ti} means the weight fraction of the single component *i*. DBE represents the double bond equivalent (Equation 4).

$$DBE = (2C - H + 2)/2 \qquad \text{Equation (4)}$$

More detailed information about the 'PM Index' is available in [25]. Aikawa et al. calculated the PM Index distribution for 1445 worldwide commercially available gasoline fuels (Fig.12 in [25]) and found that the PM Indices for the gasoline fuels sold globally fell in a very wide band, ranging from 0.67 to 3.86. If excluding the top and bottom 10% of the data, the PM Indices for the remaining 80% fuels fall into the range of 1 to 2.2. Based on the PM Index model, the fuel with the PM index value of 1 reduces the PM emissions by 54.5% compared to the fuel with a PM index value of 2.2. Given the results in the present study using a

different injection system, it appears that the difference in PM emissions made by the injection system cleanliness can be more important than that made by the gasoline fuel composition.

3.2.2. ETHANOL

Figure 16 presents the effect of injector fouling on HC emissions for ethanol at 150 bar injection pressure. Fouled injectors had a limited impact on the HC emissions from the ethanol fuelled GDI engine. Figure 17 shows the effect of injector fouling on the particulate size distributions in number (a and b) and mass (c and d) for ethanol at 4.5 and 8.5 bar IMEP at 150 bar injection pressure. Again, injector fouling had a limited impact on the particulate size distributions. It is certain that fuel impingement and fuel adsorption on the deposit near the injector tip is increased due to injector fouling. However the reason that, unlike gasoline, HC and soot formation is not increased when using ethanol is because ethanol evaporates more easily and diffusive combustion is not increased as much as when using gasoline. On the other hand, compared to the diffusive combustion of gasoline, the diffusive combustion of ethanol leads to lower HC and soot formation due to the oxygen content within the ethanol molecule.

4. CONCLUSIONS

The impact of fuel (gasoline versus ethanol) and injection system on the particle emissions has been studied in a spray guided GDI engine under the operating condition of stoichiometric air/fuel ratio, engine speed of 1500 rpm and 3.5-8.5 bar IMEP engine load. The conclusions drawn from the investigation are as follows:

1. Compared with gasoline, ethanol yielded considerably less PM emissions due to a significantly lower soot formation resulting from its oxygen content and higher volatility. Faster oxidation of ethanol-generated soot due to internal burning in the engine cylinder possibly is another reason for its low PM emissions, which requires further investigation. PN emissions from ethanol were higher than those from gasoline. This is because, unlike gasoline, most of unburnt HC from ethanol formed the nanoparticles in the nucleation mode, whilst only a small fraction of unburnt HC is attached or adsorbed on the limited soot.

2. High injection pressure improves the particle emissions from a GDI engine fuelled with gasoline, because of better spray atomization. By increasing the injection pressure from 50 bar to 150 bar, the PM and PN emissions were reduced by up to 22% and 78% respectively. Increasing the injection pressure to 172 bar further reduced the soot emission, however the PN emission was increased due to a significant increase in the nucleated HC particles. It seems that there is a trade-off between the PM and PN emissions from GDI engines at certain engine conditions.

3. Injector fouling should be considered carefully in the combustion system design for spray-guided GDI engines. Injector fouling affects the PM emissions through affecting the HC and soot formation, which itself is affected by the diffusive combustion that results from both the fuel impingement and fuel adsorption on the deposit near the injector tip. Deteriorated injectors could increase PM emissions by up to ten times as shown in this study. Unlike in the case of gasoline, the PM emissions from ethanol combustion are not affected by the injection system. The HC and soot formation are not evidently increased using low

injection pressure and when the fouled injectors are used, because ethanol evaporates more easily and thus experiences less diffusive combustion.

Furthermore, it is hypothesised that the differences in PM emissions made by injection system (pressure and injector condition) are more significant than the differences made by the composition of commercial gasoline fuels on the market. The data from Honda shows that the PM Index of 80% of worldwide commercially available gasoline fuels is within the range of 1 to 2.2, indicating a difference of up to 54.5% in the corresponding PM emissions. The difference made in PM emissions by the injection system is up to 88% in this study. However, this hypothesis requires further and comprehensive investigation.

ACKNOWLEDGMENT

This study was funded by the Royal Society International Exchange programme, Advantage West Midlands (AWM) Science City and by the National Natural Science Foundation of China (Technical Communication and Cooperative Research: 51211130117). The authors would like to acknowledge the support from Jaguar Land Rover and Shell Global Solutions UK. They also thank Peter Thornton and Carl Hingley for their technical support of the engine testing facility.

List of Tables

Table 1 Single Cylinder Engine Specification

Engine Type	4-Stroke, 4-Valve
Combustion System	Spray Guided GDI
Swept Volume	565.6 cc
Bore x Stroke	90 x 88.9 mm
Compression Ratio	11.5:1
Engine Speed	1500 rpm
DI Pressure/Injection Timing	15 MPa/280º bTDC*
Intake Valve Opening	16.5º bTDC*
Exhaust Valve Closing	36.7º aTDC*

* TDC refers to the one in the combustion stroke

Table 2 Properties of the Fuels Studied

	Gasoline	Ethanol
Chemical Formula	C_2-C_{14}	C_2H_6O
Gravimetric Oxygen Content (%)	0	34.78
Density @ 20ºC (kg/m^3)	744.6	790.9
Research Octane Number (RON)	96.8	107
Motor Octane Number (MON)	85.7	89
Stoichiometric Air-Fuel Ratio	14.46	8.95
LHV (MJ/kg)	42.9	26.9
LHV (MJ/L)	31.9	21.3
Heat of Vaporization (KJ/kg)	373	840
Initial Boiling Point (ºC)	32.8	78.4

Table 3 Engine operating conditions

Factors	Fuel	Injection Pressure (bar)	Injector number	Others
Injection pressure	gasoline	50, 100, 150, 172	# 3 (clean)	IMEP: 3.5-8.5 Lambda: 1 Engine speed: 1500 rpm, Ignition timing: MBT/KLSA
	ethanol	50, 100, 150	# 3 (clean)	
Injector fouling	gasoline	50, 150	# 1 (8.5%*) # 2 (5.3%*) # 3 (clean)	
	ethanol	150		

*The flow test results were shown in Figure 2

Table 4 Possibility of PM mode separation based on Particle size distribution expressed in number

		IMEP (bar)					
		3.5	4.5	5.5	6.5	7.5	8.5
Injection Pressure	50	-	-	-	+	++	++
	100	-	-	-	+	++	++
	150	-	-	-	-	+	++
	172	-	-	-	-	+	++

- Refers to the case of impossible mode separation

+ Refers to the case of possible mode separation however with some challenges such as in Figure 6 (b)

++ Refers to the case of very clear mode separation such as Figure 6 (a)

Table 5 Possibility of PM mode separation based on Particle size distribution expressed in mass

		IMEP (bar)					
		3.5	4.5	5.5	6.5	7.5	8.5
Injection Pressure	50	-	-	-	+	-	-
	100	-	-	-	++	-	-
	150	-	-	-	++	+	-
	172	-	-	-	++	++	+

- Refers to the case of impossible mode separation

+ Refers to the case of possible mode separation however with some challenges such as in Figure 6 (d)

++ Refers to the case Refers to the case of very clear mode separation such as Figure 6 (c)

List of Figures

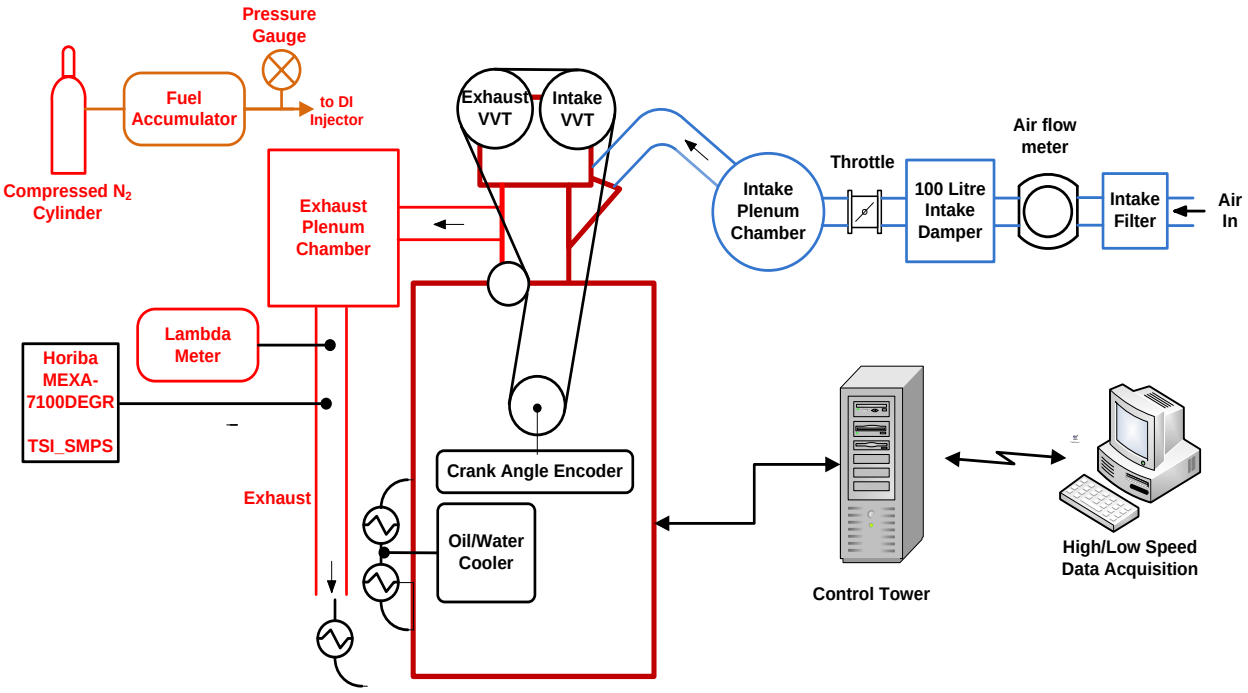

Figure 1 Schematic of Engine and Instrumentation Setup

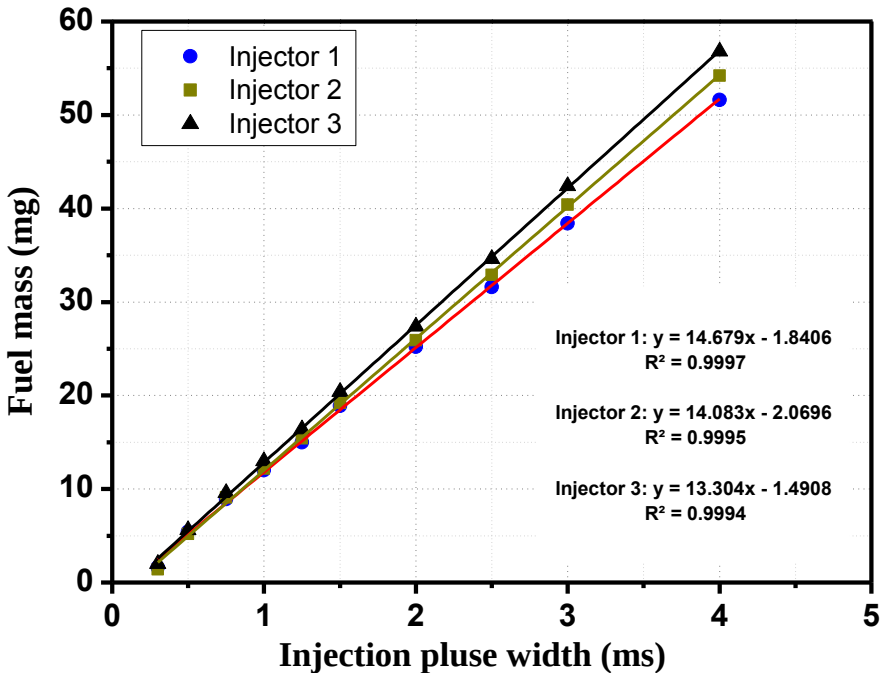

Figure 2 Injector Flow Test using iso-octane as the Test Fluid at 150 bar Injection Pressure

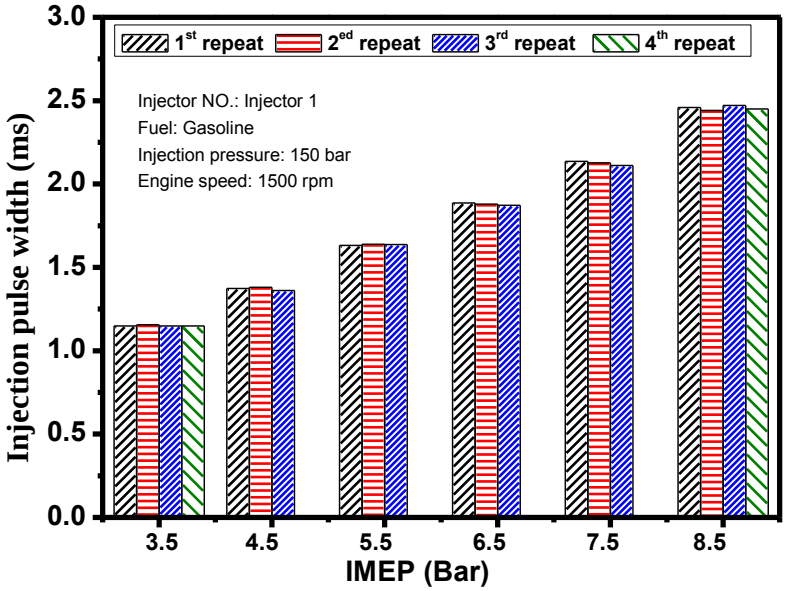

Figure 3 Injection Pulse Width for Injector 1 at 3.5-8.5 bar IMEP under 150 bar Injection Pressure during the PM Measurement

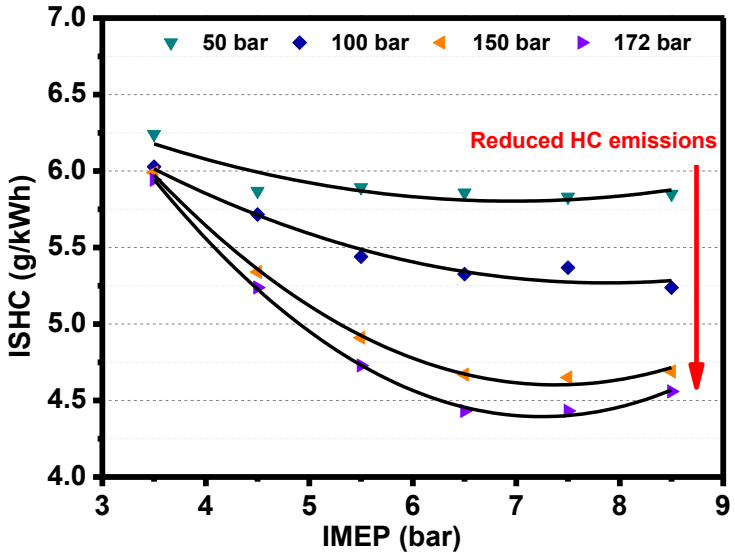

Figure 4 Effect of Injection Pressure on HC emissions in a GDI Engine Fuelled with Gasoline (engine speed=1500 rpm, λ=1)

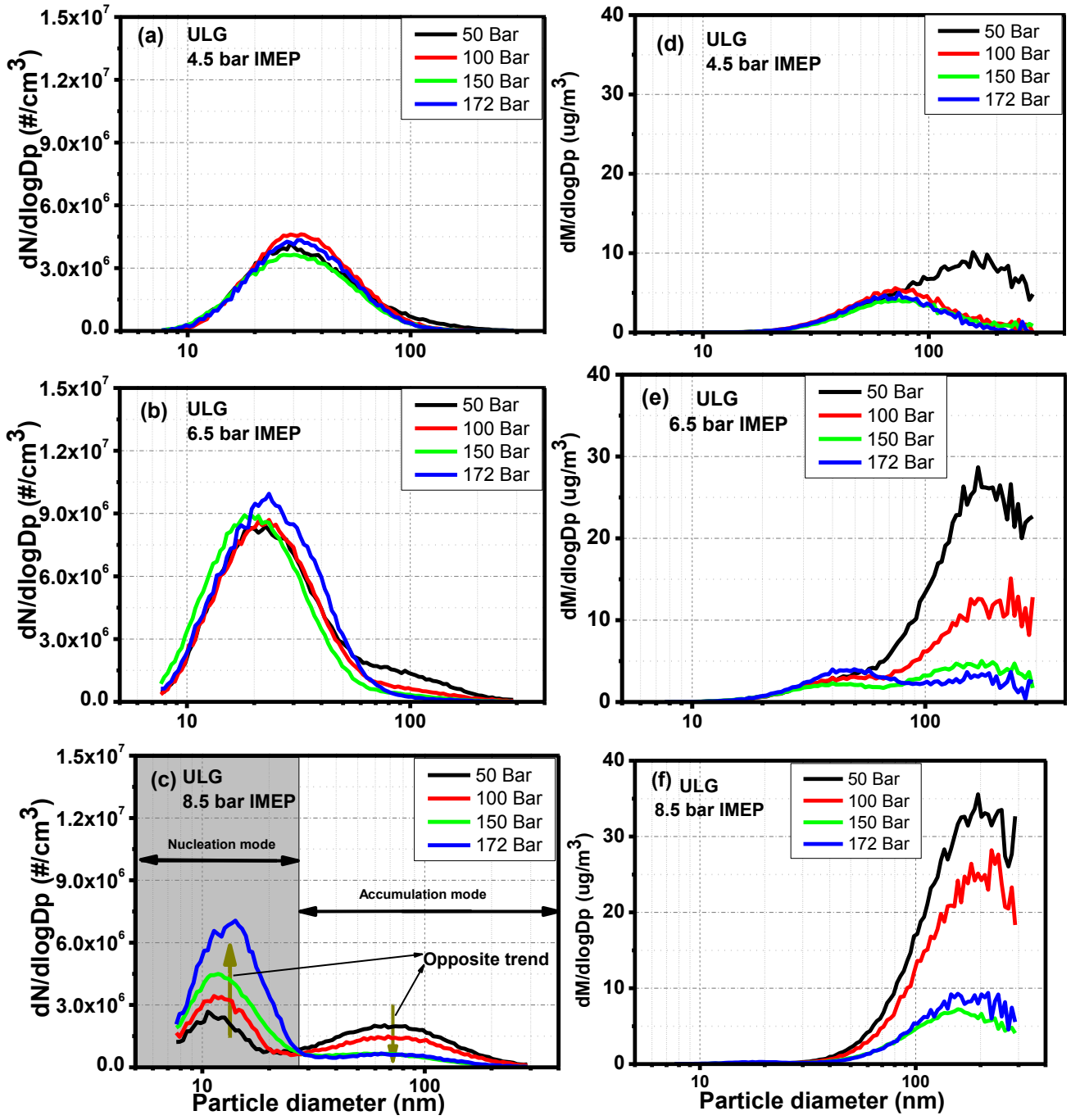

Figure 5 Effect of Injection Pressure on Particle Size Distributions in Number (a, b and c) and Mass (d, e and f) in GDI Engine Fuelled with Gasoline (engine speed=1500 rpm, λ=1)

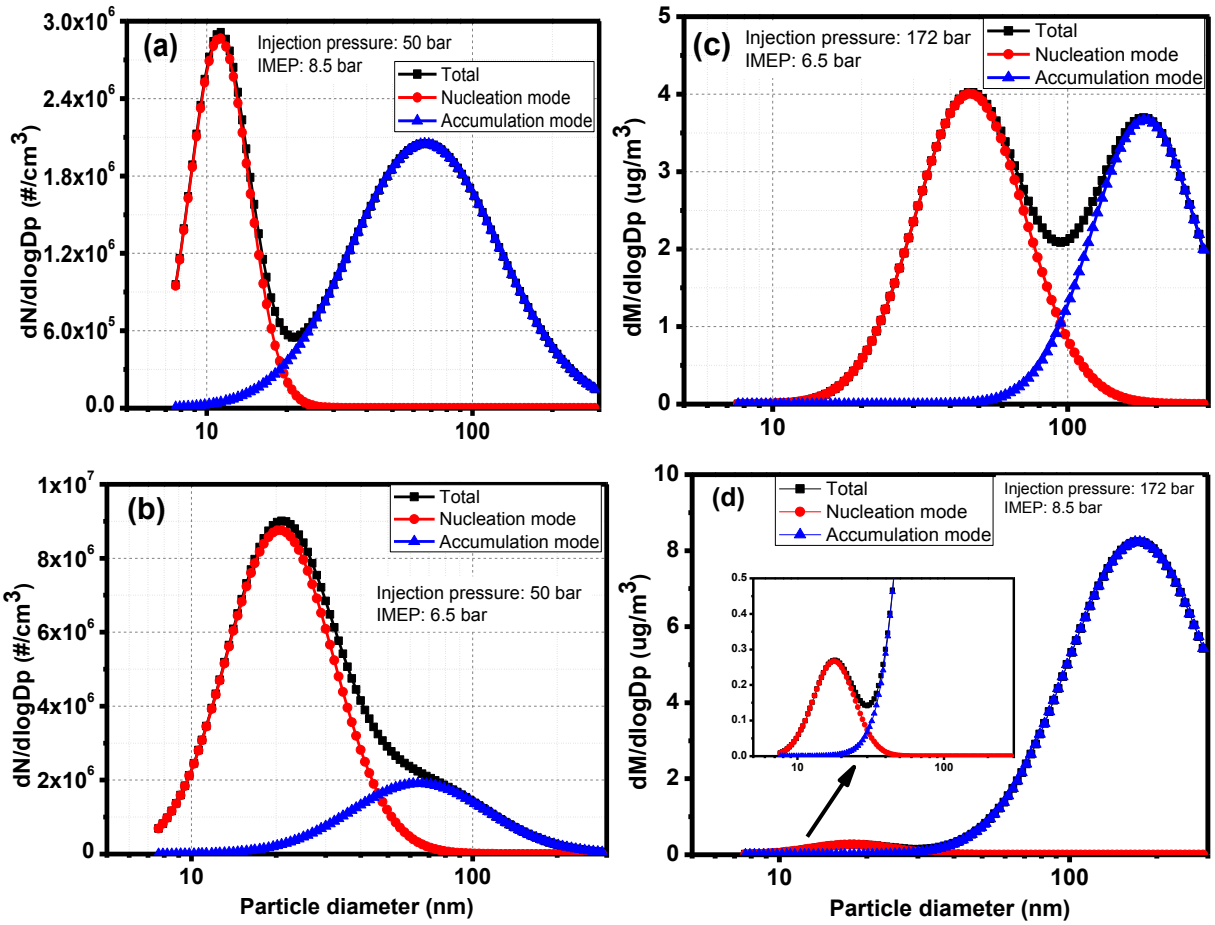

Figure 6 PM Mode Separations based on Particle Size Distributions expressed in Number (a, b) and Mass (c, d)

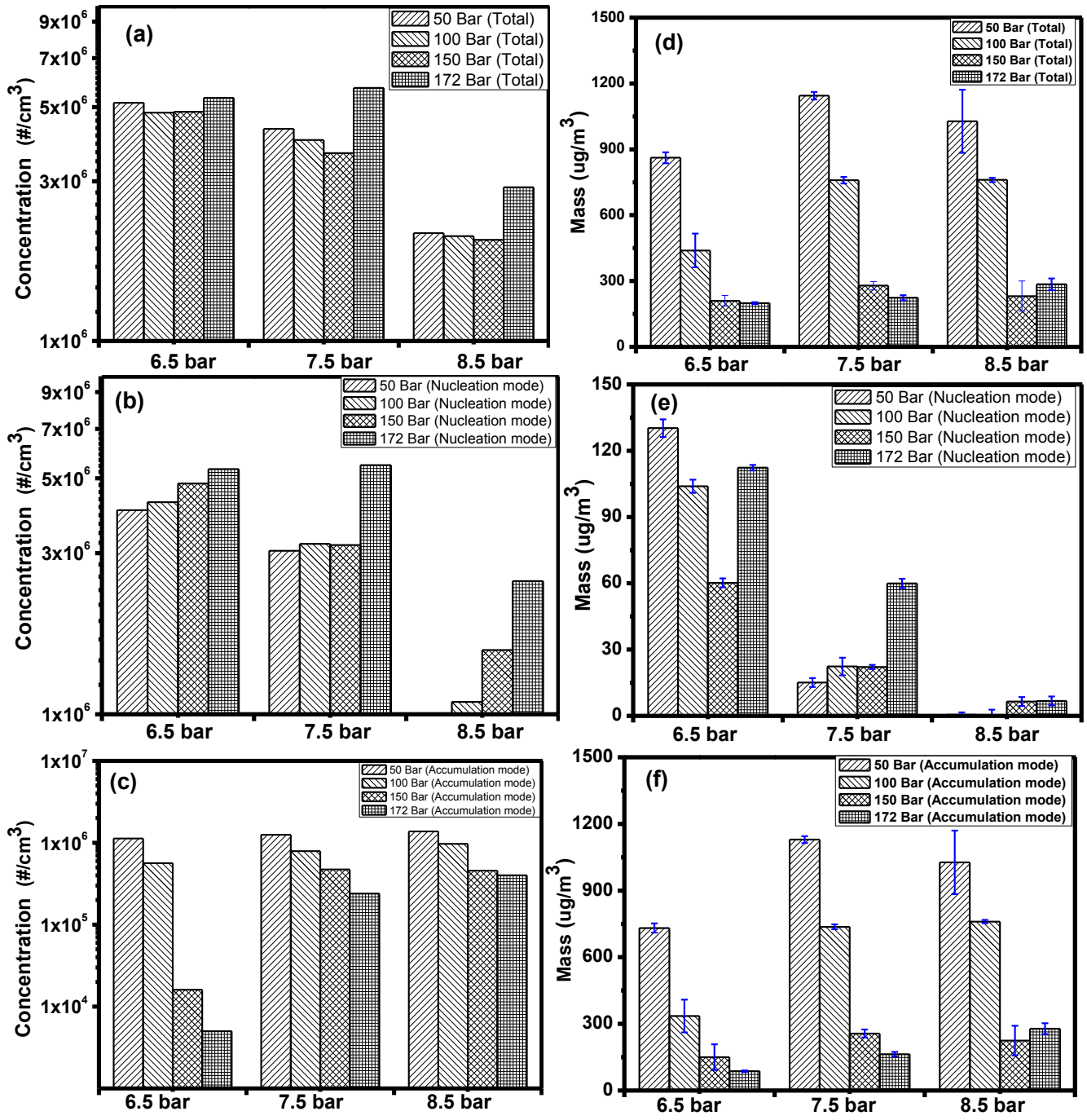

Figure 7 Effect of Injection Pressure on PN (a, b and c) and PM (d, e and f) Emissions in GDI Engine Fuelled with Gasoline (engine speed=1500 rpm, λ=1)

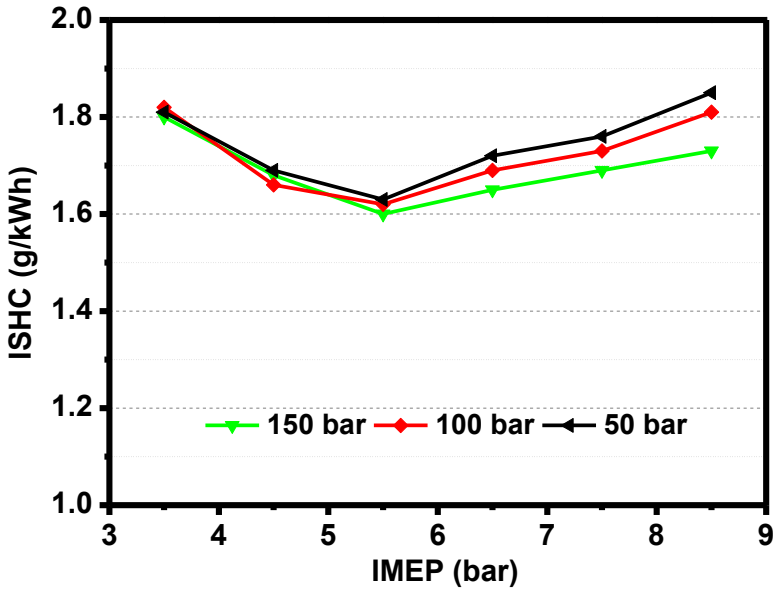

Figure 8 Effect of Injection Pressure on HC emissions in a GDI Engine Fuelled with Ethanol (engine speed=1500 rpm, λ=1)

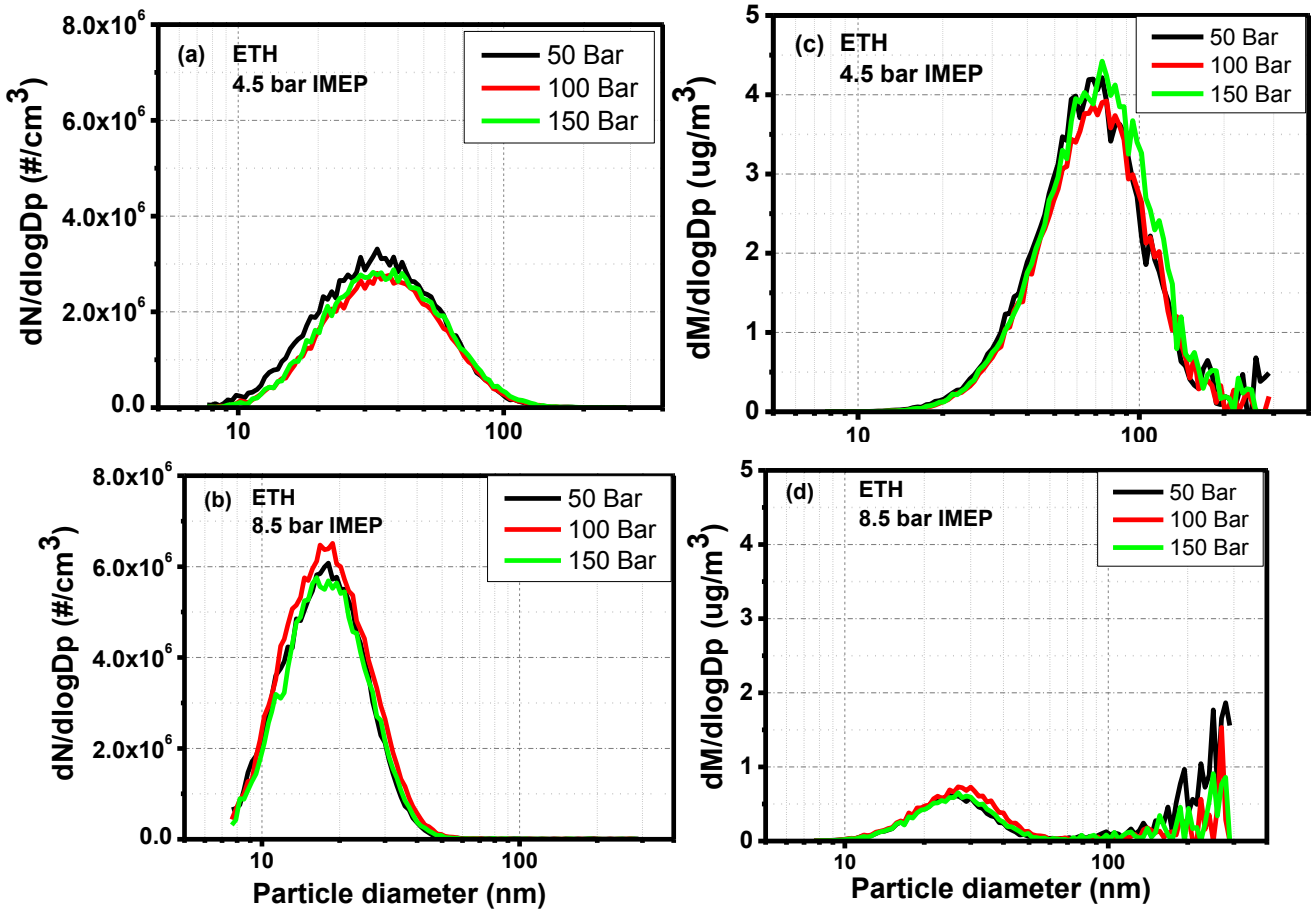

Figure 9 Effect of Injection Pressure on Particle Size distributions in Number (a, b) and Mass (c, d) in a GDI Engine Fuelled with Ethanol (engine speed=1500 rpm, λ=1)

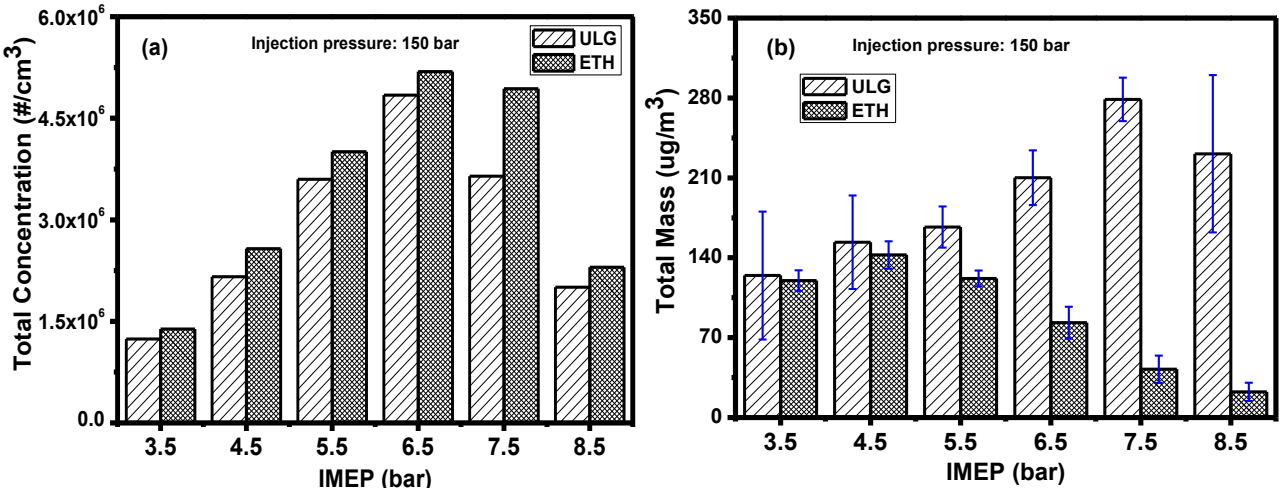

Figure 10 Comparison of (a) PN and (b) PM emissions from a GDI Engine Fuelled with Gasoline and Ethanol (engine speed=1500 rpm, λ =1)

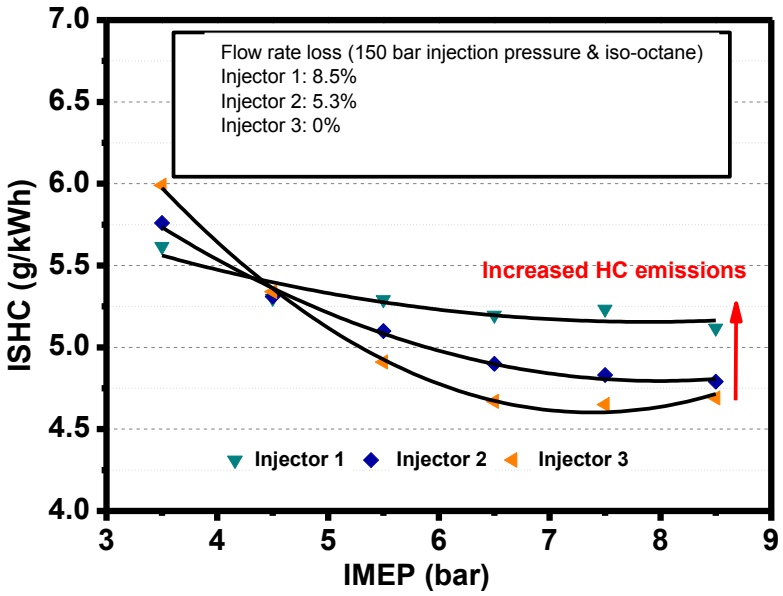

Figure 11 Effect of Injector Fouling on HC Emissions for Gasoline at 150 bar Injection Pressure (engine speed=1500 rpm, λ=1)

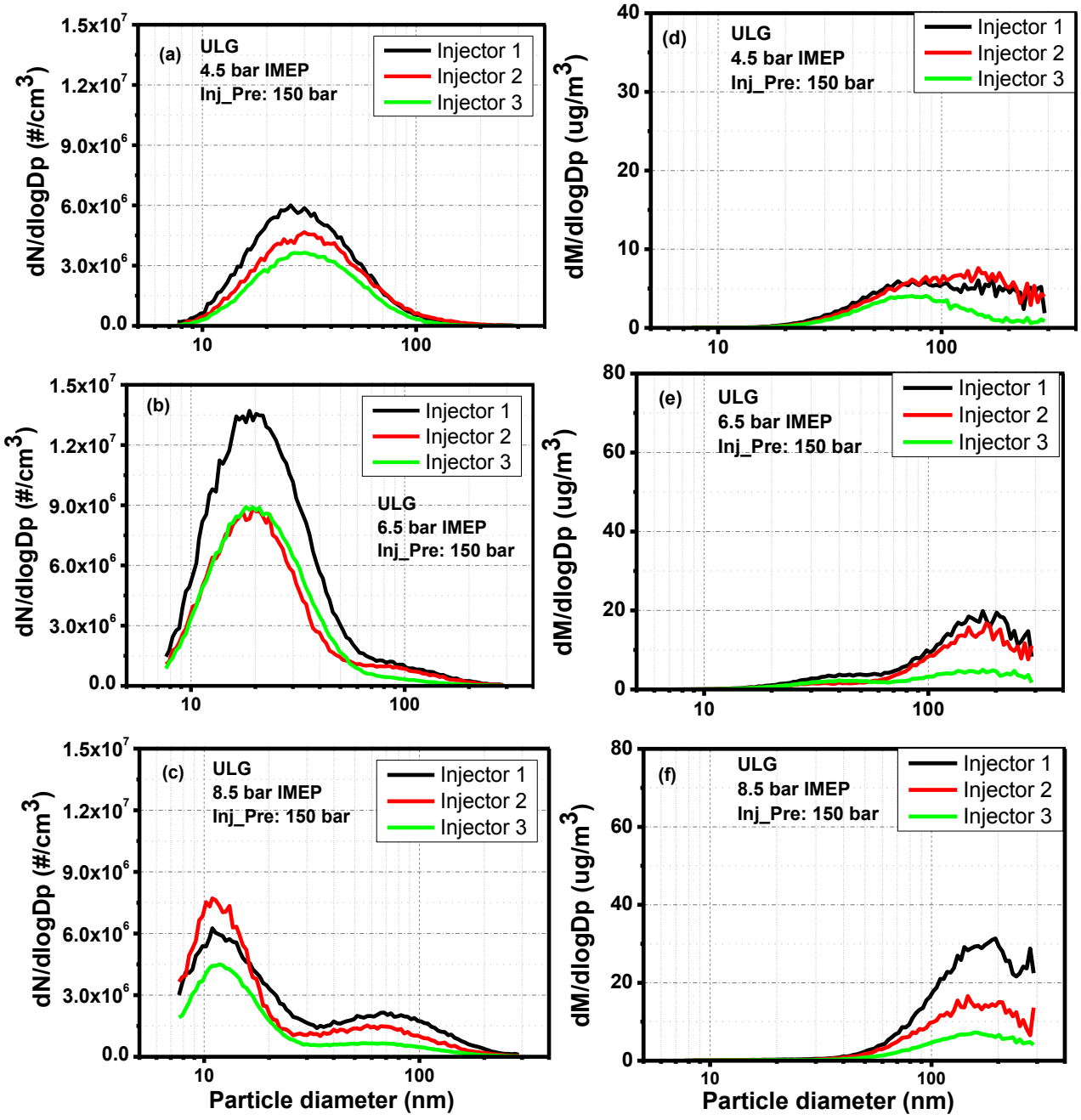

Figure 12 Effect of Injector Fouling on Particle Size distributions in Number (a, b and c) and Mass (d, e and f) in a GDI Engine Fuelled with Gasoline at 150 bar Injection Pressure (engine speed=1500 rpm, λ=1)

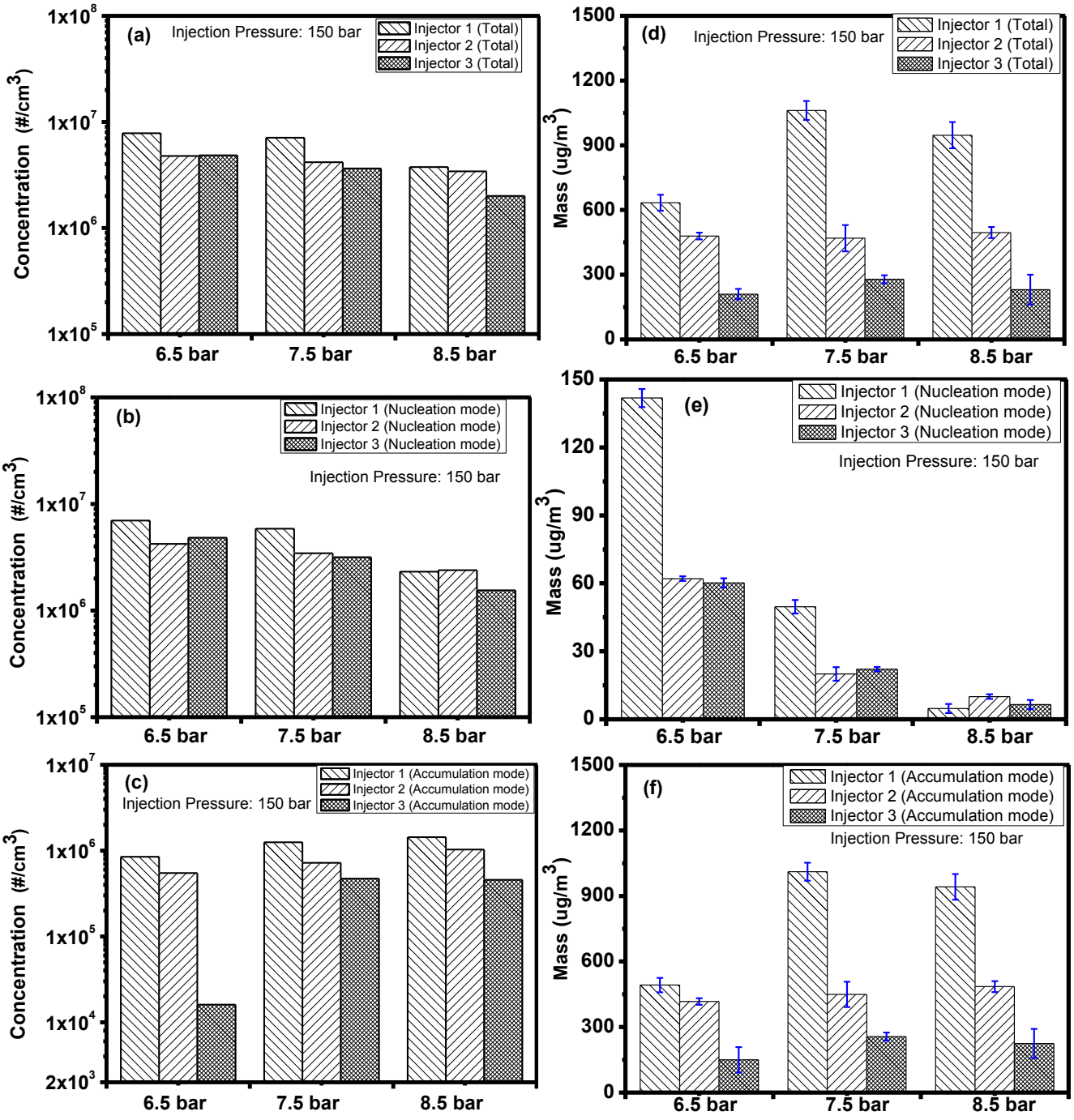

Figure 13 Effect of Injector Fouling on PN (a, b and c) and PM (d, e and f) Emissions in GDI Engine Fuelled with Gasoline at 150 bar Injection Pressure (engine speed=1500 rpm, λ=1)

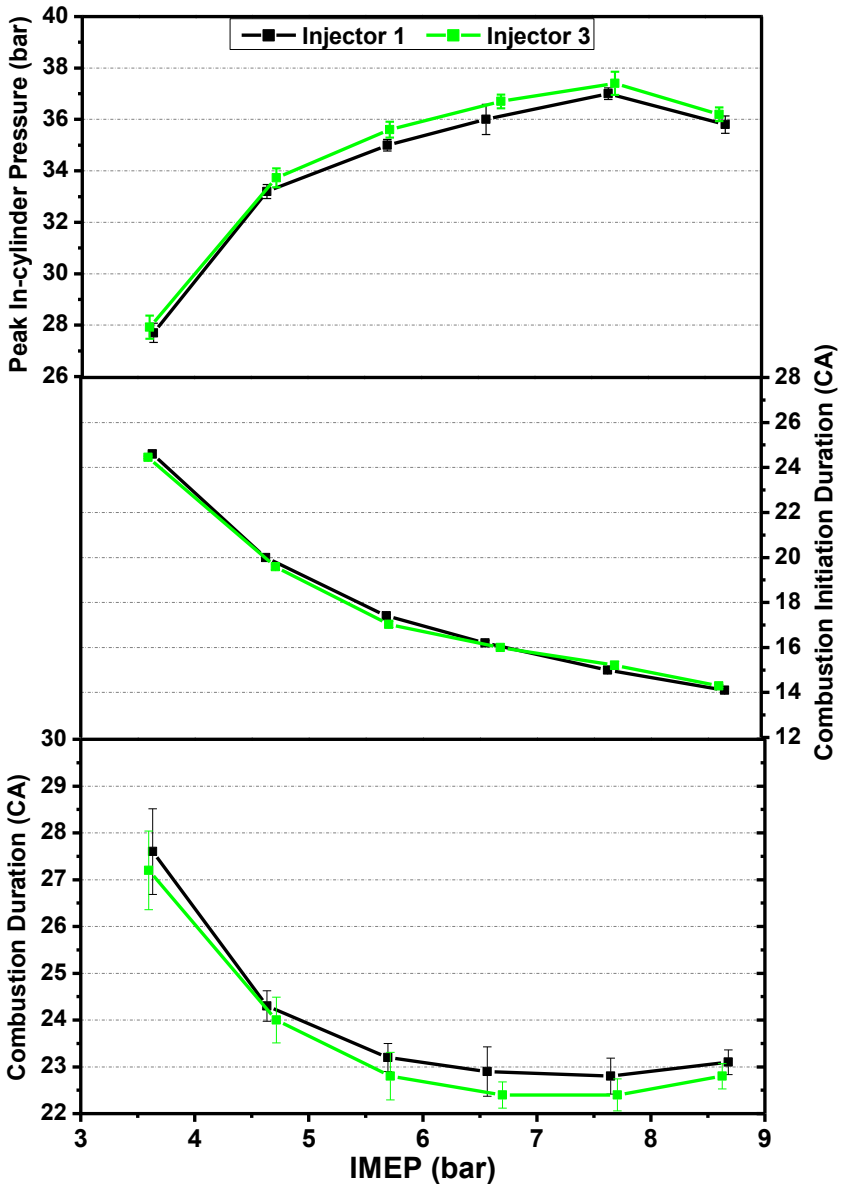

Figure 14 Peak in-cylinder Pressure, Combustion Initiation Duration (CID), and Combustion Duration for Injectors (#1) and (#3) in a GDI Engine Fuelled with Gasoline at 150 bar Injection Pressure

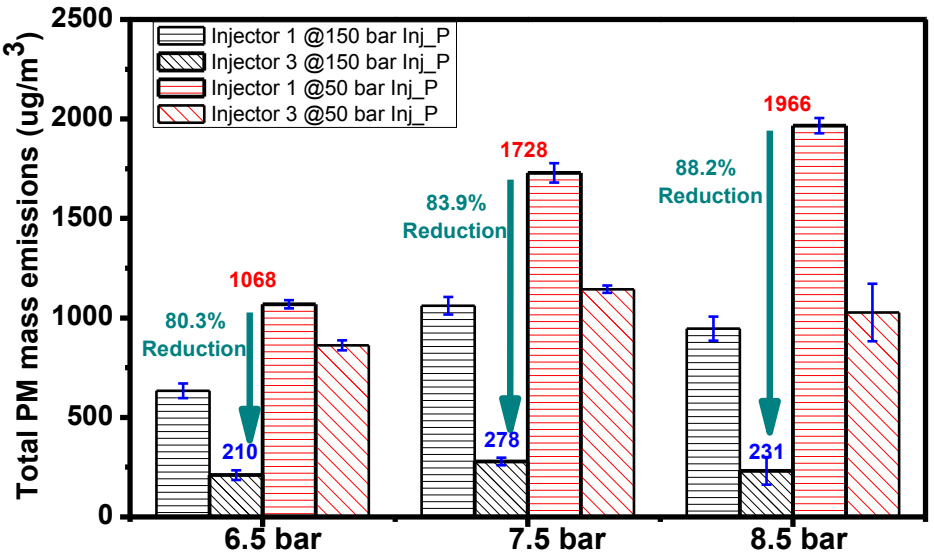

Figure 15 Comparison of total PM emissions for injectors 1 and 3 under 150 and 50 bar injection pressure at 6.5-8.5 bar IMEP

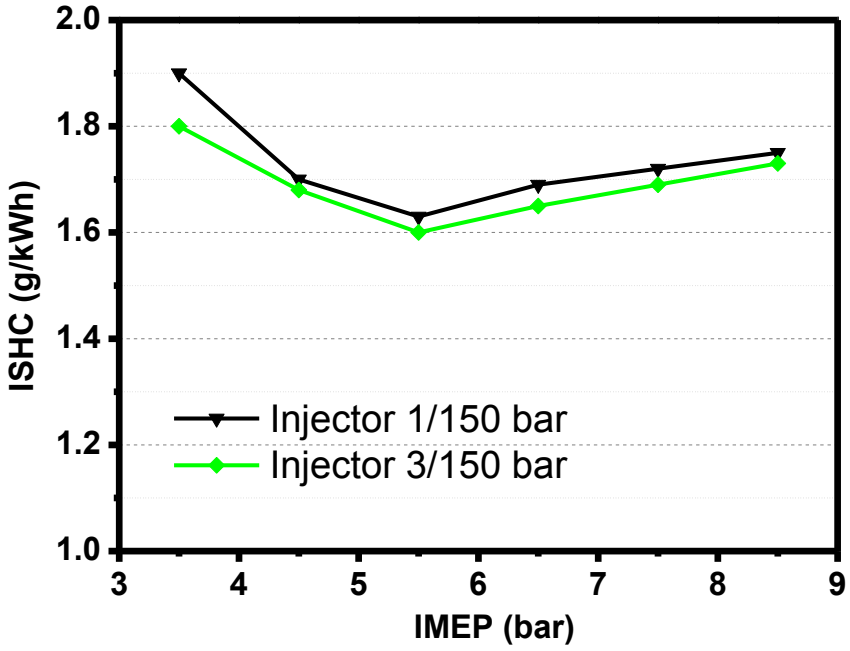

Figure 16 Effect of Injector Fouling on HC Emissions for Ethanol at 150 bar Injection Pressure (engine speed=1500 rpm, λ=1)

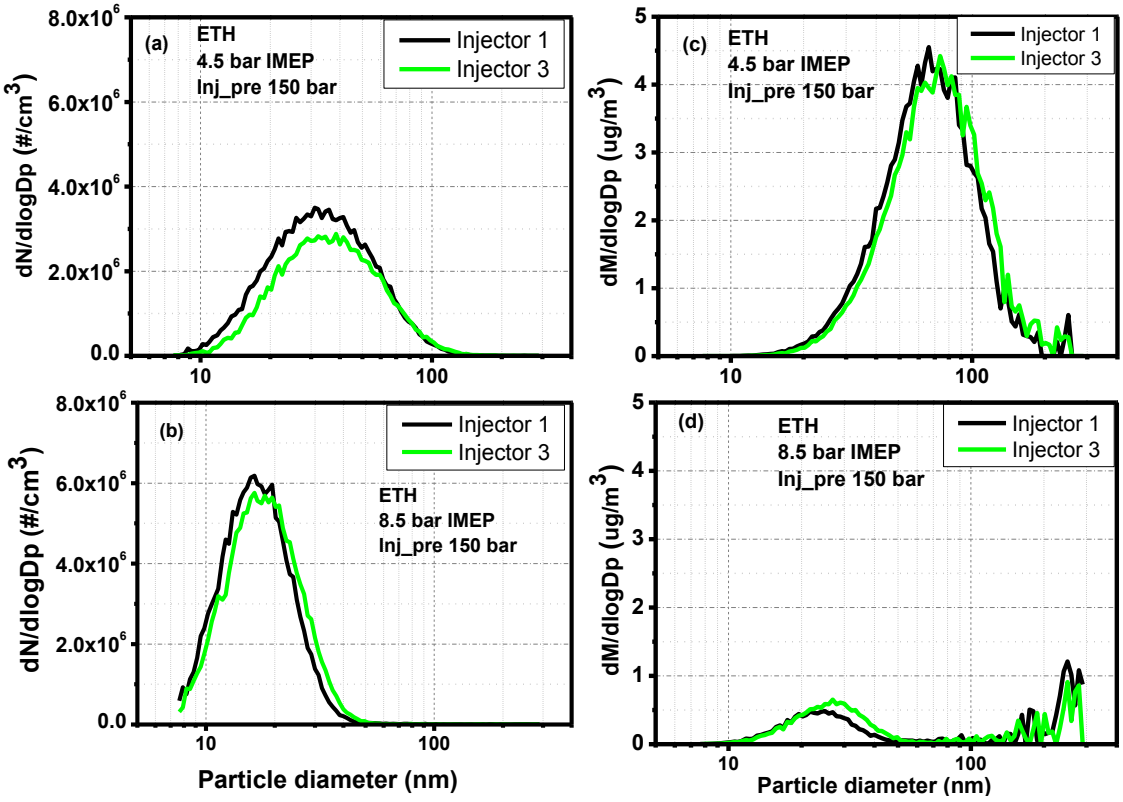

Figure 17 Effect of Injector Fouling on Particle Size Distribution in Number (a and b) and Mass (c and d) in a GDI Engine Fuelled with Ethanol at 150 bar Injection Pressure (engine speed=1500 rpm, λ=1)

DEFINITIONS, ACRONYMS, ABBREVIATIONS

AECC	Association for Emissions Control by Catalyst
AFR	Air-Fuel Ratio
AWM	Advantage West Midlands
bTDC	Before Top Dead Centre
DC	Direct Current
DI	Direct Injection
DPFs	Diesel Particulate Filters
EGR	Exhaust Gas Recirculation
EPSRC	Engineering and Physical Sciences and Research Council
ETH	Ethanol
GDI	Gasoline Direct Injection
GPFs	Gasoline Particulate Filters
HC	Hydrocarbon
IMEP	Indicated Mean Effective Pressure
MBT/KLSA	Maximum Brake Torque/ Knock-Limited Spark Advance
MON	Motor Octane Number
PID	Proportional Integral Differential
PM	Particle Mass
PN	Particulate Number
rpm	Revolutions per Minute

RON	Research Octane Number
SMPS	Scanning Mobility Particle Sizer
TDC	Top Dead Center
TWCs	Three-Way Catalysts
ULG	Gasoline

REFERENCES

[1] Zhao F, Lai MC, Harrington DL. Automotive spark-ignited direct-injection gasoline engines. Progress in Energy and Combustion Science. 1999;25:437-562.

[2] Ricardo H. Recent Research Work on the internal combustion engine. SAE Technical Paper 220001, 1922.

[3] Ando H. Combustion control for Mitsubishi GDI engine. Proceedings of the Second International Workshop on Advanced Spray Combustion, 1998.

[4] Anderson R, Brehob D, Yang J, Vallance J, Whiteaker R. A new direct injection spark ignition (DISI) combustion system for low emissions. FISITA-96, No P0201. 1996.

[5] Pontoppidan M. Experimental and numerical approach to injection and ignition optimization of lean GDI-combustion behavior. SAE Technical Paper 1999-01-0173, 1999.

[6] Ma X, Xu H, Jiang C, Shuai S. Ultra-high speed imaging and OH-LIF study of DMF and MF combustion in a DISI optical engine. Applied Energy. 2014;122:247-60.

[7] Schöppe D, Greff A, Zhang H, Frenzel H, Rösel G, Achleitner E, et al. Requirements for Future Gasoline DI Systems and Respective Platform Solutions. Internationales Wiener Motoren symoposium, 2011.

[8] Yoshida T, Sato A, Suzuki H, Tanabe T, Takahashi N. Development of High Performance Three-Way-Catalyst. SAE Technical Paper 2006-01-1061, 2006.

[9] Collins NR, Cooper JA, Morris D, Ravenscroft A, Twigg MV. Advanced Three-Way Catalysts - Optimisation by Targeted Zoning of Precious Metal. SAE Technical Paper 2005-01-2158, 2005.

[10] Bougrine S, Richard S, Michel JB, Veynante D. Simulation of CO and NO emissions in a SI engine using a 0D coherent flame model coupled with a tabulated chemistry approach. Applied Energy. 2014;113:1199-215.

[11] Wei H, Zhu T, Shu G, Tan L, Wang Y. Gasoline engine exhaust gas recirculation – A review. Applied Energy. 2012;99:534-44.

[12] Cornolti L, Onorati A, Cerri T, Montenegro G, Piscaglia F. 1D simulation of a turbocharged Diesel engine with comparison of short and long EGR route solutions. Applied Energy. 2013;111:1-15.

[13] Galindo J, Fajardo P, Navarro R, García-Cuevas LM. Characterization of a radial turbocharger turbine in pulsating flow by means of CFD and its application to engine modeling. Applied Energy. 2013;103:116-27.

[14] Zhang Z-H, Balasubramanian R. Influence of butanol addition to diesel–biodiesel blend on engine performance and particulate emissions of a stationary diesel engine. Applied Energy. 2014;119:530-6.

[15] Takada Y, Miyazaki T, Iida N. Study on local air pollution caused by NOx from diesel freight vehicle. SAE Technical Paper 2002-01-0651, 2002.

[16] Moghbelli H, Ganapavarapu K, Langari R, Ehsani M. A Comparative Review of Fuel Cell Vehicles (FCVs) and Hybrid Electric Vehicles (HEVs) Part I: Performance and Parameter Characteristics, Emissions, Well-to-Wheels Efficiency and Fuel Economy, Alternative Fuels, Hybridization of FCV, and Batteries for Hybrid Vehicles. SAE Technical Paper 2003-01-2298, 2003.

[17] Mathis U, Mohr M, Forss AM. Comprehensive particle characterization of modern gasoline and diesel passenger cars at low ambient temperatures. Atmos. Environ. 2005;39:107-17.

[18] ACSS. Particulate Emissions from Petrol-Engined Light-Duty Vehicles taken from the European Fleet. Presented in Cambridge Particle Meeting. 2013.

[19] EPA US. Integrated science assessment for particlate matter (final report). US Environmental Protection Agency, Washinton, DC, EPA/600/R-08/139F. 2009.

[20] Parkin C. Update on the UN-ECE particle measurement programme. In: Transport UDf, editor.2008.

[21] Bonatesta F, Chiappetta E, La Rocca A. Part-load particulate matter from a GDI engine and the connection with combustion characteristics. Applied Energy. 2014;124:366-76.

[22] Charlton A, Lea-Langton A, Li H, Andrews G, Tomlin A, Routledge M. Particle characteristics and DNA damage induced by exhaust particulate matter collected from a heavy duty diesel engine using biofuels. Presented in Cambridge Particle Meeting. 2011.

[23] Andersson J, Collier A, Garrett M, Wedekind B. Particle and Sulphur Species as Key Issues in Gasoline Direct Injection Exhaust. Nippon Kikai Gakkai; 1999.

[24] Price P, Stone R, OudeNijeweme D, Chen X. Cold Start Particulate Emissions from a Second Generation DI Gasoline Engine. SAE Technical Paper 2007-01-1931, 2007.

[25] Aikawa K, Sakurai T, Jetter JJ. Development of a Predictive Model for Gasoline Vehicle Particulate Matter Emissions. SAE Int J. Fuels Lubr. 2010;3:610-22.

[26] Chen L, Stone R, Richardson D. A study of mixture preparation and PM emissions using a direct injection engine fuelled with stoichiometric gasoline/ethanol blends. Fuel. 2012;96:120-30.

[27] Di Iorio S, Lazzaro M, Sementa P, Vaglieco BM, Catapano F. Particle Size Distributions from a DI High Performance SI Engine Fuelled with Gasoline-Ethanol Blended Fuels. SAE Technical Paper 2011-24-0211, 2011.

[28] Liang B, Ge Y, Tan J. Comparison of PM emissions from a gasoline direct injected (GDI) vehicle and a port fuel injected (PFI) vehicle measured by electrical low pressure impactor (ELPI) with two fuels:Gasoline and M15 methanol gasoline. Journal of Aerosol Science. 2013;57:22-31.

[29] Leach F. The Effect of Fuel Volatility and Aromatic Content on Particulate Emissions. Presented in Cambridge Particle Meeting. 2012.

[30] Armas O, García-Contreras R, Ramos Á. Impact of alternative fuels on performance and pollutant emissions of a light duty engine tested under the new European driving cycle. Applied Energy. 2013;107:183-90.

[31] Labecki L, Cairns A, Xia J, Megaritis A, Zhao H, Ganippa LC. Combustion and emission of rapeseed oil blends in diesel engine. Applied Energy. 2012;95:139-46.

[32] Khalek IA, Bougher T, Jetter JJ. Particle Emissions from a 2009 Gasoline Direct Injection Engine Using Different Commercially Available Fuels. SAE Int. J. Fuels Lubr. 2010;3:623-37.

[33] Xu F. Experimental research on particulate matter emissions from gasoline direct injection engines. PhD thesis, University of Oxford. 2012.

[34] Leach F, Stone R, Richardson D. The Influence of Fuel Properties on Particulate Number Emissions from a Direct Injection Spark Ignition Engine. SAE Technical Paper 2013-01-1558, 2013.

[35] Daniel R, Tian G, Xu H, Wyszynski ML, Wu X, Huang Z. Effect of spark timing and load on a DISI engine fuelled with 2,5-dimethylfuran. Fuel. 2011;90:449-58.

[36] Catapano F, Di Iorio S, Lazzaro M, Sementa P, Vaglieco BM. Characterization of Ethanol Blends Combustion Processes and Soot Formation in a GDI Optical Engine. SAE Technical Paper 2013-01-1316, 2013.

[37] Fatouraie M, Wooldridge M, Wooldridge S. In-Cylinder Particulate Matter and Spray Imaging of Ethanol/Gasoline Blends in a Direct Injection Spark Ignition Engine. SAE Int. J. Fuels Lubr. 2013;6:1-10.

[38] Storey JME, Barone TL, Thomas JF, Huff SP. Exhaust Particle Characterization for Lean and Stoichiometric DI Vehicles Operating on Ethanol-Gasoline Blends. SAE Technical Paper 2012-01-0437, 2012.

[39] Sherry Zhang, Wayne McMahon, Henry Toutoundjian, Manuel Cruz, Frodin B. Particulate Mass and Number Emissions from Light-duty Low Emission Gasoline Vehicles. SAE Technical Paper 2010-01-0795, 2010.

[40] Storey JM, Barone T, Norman K, Lewis S. Ethanol Blend Effects On Direct Injection Spark-Ignition Gasoline Vehicle Particulate Matter Emissions. SAE Int. J. Fuels Lubr. 2010;3:650-9.

[41] Costagliola MA, De Simio L, Iannaccone S, Prati MV. Combustion efficiency and engine out emissions of a S.I. engine fueled with alcohol/gasoline blends. Applied Energy. 2013;111:1162-71.

[42] He X, Ireland JC, Zigler BT, Ratcliff MA, Knoll KE, Alleman TL, et al. The Impacts of Mid-level Biofuel Content in Gasoline on SIDI Engine-out and Tailpipe Particulate Matter Emissions. SAE Technical Paper 2010-01-2125, 2010.

[43] Oh Y, Lee S, Kim D, Chon M, Park S. Experimental and numerical study on spray characteristics of multi-hole type GDI injectors. ILASS Americas 2012 conference; 2012.

[44] He X, Ratcliff MA, Zigler BT. Effects of Gasoline Direct Injection Engine Operating Parameters on Particle Number Emissions. Energy and Fuels. 2012;26:2014−27.

[45] Matousek T, Dageforde H, Bertsch M. Influence of injection pressures up to 300 bar on particle emissions in a GDI engine. 17th ETH Conference on Combustion Generated Nanoparticles; 2013.

[46] Aradi AA, Hotchkiss A, Imoehl B, Sayar H, Avery NL. The Effect of Fuel Composition, Engine Operating Parameters and Additives on Injector Deposits in a High-Pressure Direct injection Gasoline (DIG) Research Engine. SAE Technical Paper 1999-01-3690, 1999.

[47] Arters DC, Macduff MJ. The Effect on Vehicle Performance of Injector Deposits in a Direct Injection Gasoline Engine. SAE Technical Paper 2000-01-2021, 2000.

[48] Aradi AA, Colucci WJ, Scull HM, Openshaw MJ. A Study of Fuel Additives for Direct Injection Gasoline (DIG) Injector Deposit Control. SAE Technical Paper 2000-01-2020, 2000.

[49] Jackson NS, Stokes J, Whitaker PA. A gasoline direct injection (GDI) powered vehicle concept with 3 litre/ 100 km fuel economy and EC stage 4 emission capability. Proceedings of the EAEC 6th European Congress, 1997.

[50] Bardasz EA, Arters DC, Schiferl EA, Righi DW. A Comparison of Gasoline Direct Injection and Port Fuel Injection Vehicles: Part II - Lubricant Oil Performance and Engine Wear. SAE Technical Paper 1999-01-1499, 1999.

[51] Aradi AA, Evans J, Miller K, Hotchkiss A. Direct Injection Gasoline (DIG) Injector Deposit Control with Additives. SAE Technical Paper 2003-01-2024, 2003.

[52] Joedicke A, Krueger-Venus J, Bohr P, Cracknell R, Doyle D. Understanding the Effect of DISI Injector Deposits on Vehicle Performance. SAE Technical Paper 2012-01-0391, 2012.

[53] Sandquist H, Denbratt I, Owrang F, Olsson J. Influence of Fuel Parameters on Deposit Formation and Emissions in a Direct Injection Stratified Charge SI Engine. SAE Technical Paper 2001-01-2028, 2001.

[54] Berndorfer A, Breuer S, Piock W, Bacho PV. Diffusion Combustion Phenomena in GDi Engines caused by Injection Process. SAE Technical Paper 2013-01-0261, 2013.

[55] Bacho PSV, Sofianek JK, Galante-Fox JM, McMahon CJ. Engine Test for Accelerated Fuel Deposit Formation on Injectors Used in Gasoline Direct Injection Engines. SAE Technical Paper 2009-01-1495, 2009.

[56] Kinoshita M, Saito A, Matsushita S, Shibata H, Niwa Y. A Method for Suppressing Formation of Deposits on Fuel Injector for Direct Injection Gasoline Engine. SAE Technical Paper 1999-01-3656, 1999.

[57] Katashiba H, Honda T, Kawamoto M, Sumida M, Fukutomi N, Kawajiri K. Improvement of center injection spray guided DISI performance. SAE Technical Paper 2006-01-1001, 2006.

[58] Symonds J, Price P, Williams P, Stone R. Density of particles emitted from a gasoline direct injection engine. 12th ETH-Conference on Combusiton Generated Nanoparticles, 2008.

[59] Kittelson DB. Engines and nanoparticles: A review. Journal of Aerosol Science. 1998;29:575-88.

[60] Maricq MM, Podsiadlik DH, Brehob DD, Haghgooie M. Particulate Emissions from a Direct-Injection Spark-Ignition (DISI) Engine. SAE Technical Paper 1999-01-1530, 1999.

[61] Farron C, Matthias N, Foster D, Andrie M, Krieger R, Najt P, et al. Particulate Characteristics for Varying Engine Operation in a Gasoline Spark Ignited, Direct Injection Engine. SAE Technical Paper 2011-01-1220, 2011.

[62] Myung C-L, Kim J, Choi K, Hwang IG, Park S. Comparative study of engine control strategies for particulate emissions from direct injection light-duty vehicle fuelled with gasoline and liquid phase liquefied petroleum gas (LPG). Fuel. 2012;94:348-55.

[63] Ojapah MM, Zhang Y, Zhao H. Analysis of Gaseous and PM Emissions of 4-Stroke CAI/HCCI and SI Combustion in a DI Gasoline Engine. SAE Technical Paper 2013-01-1549, 2013.

[64] Daniel R, Tian G, Xu H, Wu X. Spark Timing Sensitivity of Gasoline, Ethanol and 2,5-Dimethylfuran in a DISI Engine. Fuel. 2012;99:72-82.

[65] Daniel R, Xu H, Wang C, Richardson D, Shuai S. Gaseous and particulate matter emissions of biofuel blends in dual-injection compared to direct-injection and port injection. Applied Energy. 2013;105:252-61.

[66] Eastwood P. Particulate Emissions from Vehicles: John Wiley & Sons, Inc.; 2007.

[67] Armas O, Gomez A, Mata C. Methodology for measurement of diesel particle size distributions from a city bus working in real traffic conditions. Meas. Sci. Technol. 2011;22.

[68] Li H, li C, Ma X, Tu P, Xu H, Shuai S-J, et al. Numerical Study of DMF and Gasoline Spray and Mixture Preparation in a GDI Engine. SAE Technical Paper 2013-01-1592, 2013.

[69] Tian G, Li H, Xu H, Li Y, Raj SM. Spray Characteristics Study of DMF Using Phase Doppler Particle Analyzer. SAE Int. J. Passeng Cars – Mech. Syst. 2010;3:948-58.

[70] Wang C, Xu H, Herreros JM, Lattimore T, Shuai S. Fuel Effect on Particulate Matter Composition and Soot Oxidation in a Direct-Injection Spark Ignition (DISI) Engine. Energy & Fuels. 2014;28:2003-12.

[71] Lindgren R, Skogsberg M, Sandquist H, Denbratt I. The Influence of Injector Deposits on Mixture Formation in a DISC SI Engine. SAE Technical Paper 2003-01-1771, 2003.

[72] Ashida T, Takei Y, Hosi H. Effects of Fuel Properties on SIDI Fuel Injector Deposit. SAE Technical Paper 2001-01-3694, 2001.

[73] DuMont RJ, Evans JA, Feist DP, Studzinski WM, Cushing TJ. Test and Control of Fuel Injector Deposits in Direct Injected Spark Ignition Vehicles. SAE Technical Paper 2009-01-2641 2009.

[74] Taniguchi S, Yoshida K, Tsukasaki Y. Feasibility Study of Ethanol Applications to A Direct Injection Gasoline Engine Journal. SAE Technical Paper 2007-01-2037, 2007.

[75] Heywood JB. Internal combustion engine fundamentals: McGraw-Hill: New York; 1989.